RESEARCH ARTICLE

P-glycoprotein Detoxification by the Malpighian Tubules of the Desert Locust

Marta Rossi[1]*, Davide De Battisti[2] and Jeremy E. Niven[1,3*]

[1]School of Life Sciences, University of Sussex, Falmer, Brighton BN1 9QG, UK

[2]Department of Bioscience, Swansea University, Swansea, Singleton park SA2 8PP, Wales, UK

[3]Centre for Computational Neuroscience and Robotics, University of Sussex, Falmer, Brighton BN1 9QG, UK

*Authors for correspondence (M.Rossi@sussex.ac.uk and J.E.Niven@sussex.ac.uk)

KEYWORDS: ABC transporter, rhodamine B, verapamil, *Schistocerca gregaria*, mixed effects model, transepithelial transport, net extrusion

ABSTRACT

Detoxification is essential for allowing animals to remove toxic substances present in their diet or generated as a biproduct of their metabolism. By transporting a wide range of potentially noxious substrates, active transporters of the ABC transporter family play an important role in detoxification. One such class of transporters are the multidrug resistance P-glycoprotein transporters. Here, we investigated P-glycoprotein transport in the Malpighian tubules of the desert locust (*Schistocerca gregaria*), a species whose diet includes plants that contain toxic secondary metabolites. To this end, we studied transporter physiology using a modified Ramsay assay in which *ex vivo* Malpighian tubules are incubated in different solutions containing the P-glycoprotein substrate dye rhodamine B in combination with different concentrations of the P-glycoprotein inhibitor verapamil. Our evidence shows that: (i) the Malpighian tubules contain a P-glycoprotein; (ii) tubule surface area is positively correlated with the tubule fluid secretion rate; and (iii) as the fluid secretion rate increases so too does the net extrusion of rhodamine B. We were able to quantify precisely the relationships between the fluid secretion, surface area, and net extrusion. We interpret these results in the context of the life history and foraging ecology of desert locusts. We argue that P-glycoproteins play an important role in the detoxification by contributing to the removal of xenobiotic substances from the haemolymph, thereby enabling gregarious desert

locusts to maintain toxicity through the ingestion of toxic plants without suffering the deleterious effects themselves.

INTRODUCTION

Insect excretory systems consist primarily of the Malpighian tubules and the hindgut, which act synergistically to regulate haemolymph composition (e.g. Maddrell *et al.,* 1974; Ramsay, 1958). Malpighian tubules are blind ended tubules that float in the haemolymph and empty into the gut at the midgut-hindgut junction, secreting primary urine, the composition of which is modified by water and ion reabsorption in the hindgut (Phillips, 1964). The tubules are considered analogous to vertebrate nephrons (Ramsay, 1958). Cells of the epithelium forming the tubule wall express primary and secondary active transporters that move K^+, Na^+ and Cl^- ions into the lumen creating an osmotic gradient that produces water secretion (for a review see O'Donnell, 2008). Insects regulate ion and water secretion according to their feeding habits and ecological niche. For example, haematophagous insects must cope with an excess of NaCl and water after a blood meal (Williams *et al*., 1983), whereas phytophagous insects must often cope with a diet rich in K^+ as well as with secondary metabolites (Maddrell and Klunsuwan, 1973; Wieczorek, 1992).

In addition to osmoregulation, Malpighian tubules play a fundamental role in the removal of metabolic waste and potentially noxious substances that have been ingested (Maddrell and Gardiner, 1976; Maddrell *et al.*, 1974). Alkaloids and organic anions and cations are actively transported by ATP-dependant transporters such as the multidrug resistance-associated protein 2 (MRP2) and P-glycoproteins (P-gps, multidrug resistance protein (MDR1) or ABCB1), both members of the ABC transporter family (Gaertner *et al*., 1998; Karnaky Jr *et al*., 2000). Multidrug resistance-associated protein 2 (MRP2) transporters are involved in the transport of organic anions (Leader and O'Donnell, 2005; O'Donnell and Leader, 2006), while P-glycoproteins transport type II organic cations (>500 Da), hydrophobic and often polyvalent compounds (e.g. alkaloids and quinones) (Wright and Dantzler, 2004).

The presence and physiology of these multidrug transporters have been explored using specific substrates and selective inhibitors (e.g. Gaertner *et al*., 1998; Hawthorne and Dively, 2011; Leader and O'Donnell, 2005). In the Malpighian tubules of the cricket (*Teleogryllus commodus*) and the fruit fly (*Drosophila melanogaster*), the transepithelial transport of the fluorescent MRP2 substrate Texas Red is reduced by the MRP2 inhibitors MK571 and probenecid (Leader and O'Donnell, 2005), while the transport of the fluorescent P-glycoprotein substrate daunorubicin is selectively reduced by the P-glycoprotein inhibitor verapamil (Leader and O'Donnell, 2005). The transport of nicotine by P-glycoprotein transporters has also been demonstrated in numerous insect species, including the tobacco

71 hornworm (*Manduca sexta*; Gaertner *et al*., 1998), fruit fly (*D. melanogaster*), kissing bug
72 (*Rhodnius prolixus*), large milkweed bug (*Oncopeltus fasciatus*), yellow fever mosquito (*Aedes*
73 *aegypti*), house cricket (*Acheta domesticus*), migratory locust (*Locusta migratoria*), mealworm
74 beetle (*Tenebrio molitor*), American cockroach (*Periplaneta americana*) and cabbage looper
75 (*Trichoplusia ni*) (Rheault *et al*., 2006). In insects, the understanding of the interaction between
76 xenobiotics (i.e. insecticides, herbicides, miticides and secondary plant metabolites) and P-
77 glycoprotein transporters is still limited, but there is an increasing interest in understanding
78 how different xenobiotics can act synergistically to maximize the efficacy of insecticides in
79 pests or impair the xenobiotic detoxification if beneficial insects such as honey bees (Guseman
80 *et al*., 2016).

81 Desert locusts (*Schistocerca gregaria*) are generalist phytophagous insects with
82 aposematic coloration in the gregarious phase. They feed on a wide range of plants including
83 those, such as *Schouwia purpurea* and *Hyoscyamus muticus*, that contain toxins to become
84 unpalatable for and toxic to predators (Despland and Simpson, 2005; Mainguet *et al*., 2000;
85 Sword *et al*., 2000; for a review see Pener and Simpson, 2009). Nevertheless, it is likely that
86 gregarious desert locusts excrete some of the toxins that they ingest, relying instead on their
87 gut contents to maintain toxicity (Sword, 2001, 1999). Two lines of evidence suggest that this
88 excretion is likely to involve P-glycoproteins: (1) they are expressed in the Malpighian tubules
89 of numerous species (e.g. *A. domesticus, L. migratoria, P. americana*) from orthopteroid
90 orders (Rheault *et al*., 2006); and (2) they are expressed in the blood brain barrier of the desert
91 locust (Andersson *et al*., 2014). However, P-glycoproteins in the Malpighian tubules of desert
92 locusts have not been studied previously.

93 Here we show that xenobiotic transport and extrusion in the Malpighian tubules of the
94 desert locust is an active process dependent upon P-glycoprotein like transporters using
95 isolated tubules to perform a modified Ramsay secretion assay (Ramsay, 1954). We
96 evaluated the extrusion of the P-glycoprotein substrate dye rhodamine B (e.g. Eytan *et al*.,
97 1997; Mayer *et al*., 2009) with or without the addition of the selective P-glycoprotein inhibitor
98 verapamil (e.g. Andersson *et al*., 2014; Dermauw and Van Leeuwen, 2014; Hamada *et al.*,
99 1987). Our results suggest that P-glycoprotein transporters may play an important role in the
100 xenobiotic detoxification in the Malpighian tubules of the desert locust. By using linear mixed
101 effect models to account for repeated observations of single tubules and obtaining multiple
102 tubules from single locusts, we found that tubule surface area more accurately predicts fluid
103 secretion rate than diameter or length. Moreover, this statistical model allowed us to quantify
104 the influence of the surface area on the fluid secretion rate in different treatments, and how it
105 changes over time. We found that the surface area of the tubules positively influences their
106 fluid secretion rate and that the fluid secretion rate influences the net extrusion of rhodamine

107 B. We propose that this assay may be used in future to understand the physiology of the P-
108 glycoproteins when exposed to a wide range of different substances.
109

110 MATERIALS AND METHODS

111 **Animals**

112 Fifth instar desert locusts (*Schistocerca gregaria;* Forskål, 1775) were obtained from
113 Peregrine Livefoods (Essex, UK) and raised under crowded conditions at 28-30°C with 12:12
114 photoperiod. Locusts were fed with organic lettuce, fresh wheat seedlings and wheat germ *ad*
115 *libitum*. Fifth instar nymphs were checked daily and, within 24 hours post-eclosion, were
116 marked with acrylic paint (Quay Imports Ltd, Kirkham, Lancashire, UK). Only adult males
117 between 20 and 22 days post-eclosion were used in the experiments.
118

119 **Saline and chemicals**

120 The saline used was adapted from the Ringer solution of Maddrell and Klunsuwan (1973). Its
121 composition was: 5.73 g/L NaCl (98 mM), 0.30 g/L KCl (4 mM), 2 mL $CaCl_2$ solution 1M (2
122 mM), 1.86 g/L $NaHCO_3$ (22 mM), 1.09 g/L $NaH_2P0_4{\cdot}2H_2O$ (7 mM), 0.19 g/L $MgCl_2$ (2 mM),
123 1.80 g/L glucose (10 mM), 0.83 g/L sodium glutamate (4.9 mM), 0.88 g/L sodium citrate (3.5
124 mM) and 0.37 g/L malic acid (2.8 mM). The final pH of the saline was 7.15. It was stored at
125 4°C for a maximum of three days. Stock solutions of rhodamine B (50 mM and 3 mM) and
126 verapamil hydrochloride (20 mM) were prepared in water and diluted to the final concentration
127 in the saline. Rhodamine B was applied at 60 µM and verapamil at 125 µM or 250 µM. All
128 chemicals were purchased from Sigma-Aldrich (UK) or Fisher Scientific (UK).
129

130 **Locust dissection**

131 The locusts were placed in the freezer for 4-5 minutes until sedated. Upon removal from the
132 freezer, the abdomen was cut transversely ~5 mm from the anus, and holding the head with
133 one hand and the thorax with the other hand, the head was pulled away from the remainder
134 of the body (Figure 1A) (Maddrell and Klunsuwan, 1973). In this way, the entire gut with the
135 Malpighian tubules attached was removed from the body. The gut was placed onto an 8 cm
136 Sylgard® 184 (Dow Corning, Midland, MI, USA) coated Petri dish, filled with saline. The head
137 was separated from the saline using modelling clay (Plasticine®) (Figure 1B). The preparation
138 was pinned at the cut distal end of the gut to prevent it from floating.
139

140 **Malpighian tubules dissection**

141 Using a Nikon SMZ-U (Nikon Corp., Tokyo, Japan) stereoscopic microscope, the Malpighian
142 tubules were removed by gently pulling the distal part to release them from the trachea and

cutting the proximal end at ~5 mm from the gut. Each isolated tubule was moved immediately into a 30 µL drop of saline on a 5 cm Sylgard® coated Petri dish and covered with paraffin oil to prevent desiccation. Both ends of each Malpighian tubule were pulled out from the saline drop in opposite directions and wrapped around steel pins pushed into the Sylgard® layer (Figure 1C). Three anterior tubules were removed from each locust.

Fluid secretion (Ramsay) assay

Using a sharpened glass capillary tube, each tubule was punctured near the proximal end to allow the fluid secretion (Figure 2A). The first droplet secreted immediately after puncturing was discarded. After 30 minutes of preincubation in the saline bath, the secreted droplet was removed (Figure 2B) using a P10 pipette (Gilson Scientific UK, Dunstable, Bedfordshire, UK) and photographed with a digital camera (Canon EOS 7D; Canon, Tokyo, Japan) mounted with two custom attachments (Best scientific A clamp via 1.6 x Canon mount; Leica 10445930 1.0 x) on the stereoscopic microscope (Nikon SMZ-U; Nikon Corp., Tokyo, Japan). Images were shot in raw format and processed with ImageJ v.1.51p software (Schneider *et al.,* 2012). The saline bath was then replaced with 30 µL drop containing one of the four different treatments we tested: (i) saline, (ii) rhodamine B 60 µM, (iii) rhodamine B 60 µM + verapamil 125 µM, (iv) rhodamine B 60 µM + verapamil 250 µM (Figure 2C). Again, the first droplet secreted after drop replacement was discarded. For the subsequent 90 minutes, the secreted droplet was removed at intervals of 30 minutes and photographed (Figure 2D). To prevent the photobleaching of the rhodamine B, we minimised light exposure by conducting the experiment under red light and keeping the sample in a custom designed dark box between measurements.

Droplet measurement

The diameter (µm) of each secreted droplet (Figure 3A) was measured to permit its volume (nL) to be calculated using the sphere formula, where V is the drop volume and d the droplet diameter. The volume was converted from µm^3 to nL using the following formula:

$$V = \frac{4}{3}\pi\left(\frac{d}{2}\right)^3 10^{-6}$$

For each tubule, we calculated the fluid secretion rate (nL/min), given by the droplet volume divided by the time between samples (30 mins). For each droplet, we also measured colour intensity to estimate the rhodamine B concentration (µM) from a calibration curve (see below). To estimate the number of moles of rhodamine B extruded per minute, we calculated the net extrusion of rhodamine B (fmol/min) as the product of the secretion rate and the rhodamine B concentration.

Rhodamine B calibration curve

The intensity of the droplets depends not only on rhodamine B concentration, but also on the droplet diameter (see Supplemental Methods; Supplemental Figure 1,2). So, we constructed a calibration curve for rhodamine B concentration to estimate the rhodamine B concentration of the droplets secreted. We prepared standard solutions of known rhodamine B concentrations: 0, 15, 30, 50, 60, 75, 120, 150, 240 and 480 µM. For each concentration, droplets of different sizes were placed on a Petri dish coated with Sylgard® and covered with paraffin oil. We photographed the droplets against a white background at the same light intensity, and white balancing the camera before shooting. All the images were analysed subsequently using ImageJ v.1.51p software (Schneider *et al.,* 2012).

Droplet colour varied from white (transparent droplet at rhodamine B concentration = 0 µM) to intense pink, depending upon the rhodamine B concentration. We split each image into the component colour channels and measured the intensity of the green channel. To control for the background, we compared the mean intensity inside the droplet with that outside (Figure 3B) using the formula:

$$I = I_i - I_o$$

where I is the intensity, I_i is the intensity inside the droplet, and I_o is the intensity outside the droplet. We used a range of droplet diameters from 138 to 999 µm.

To validate the reliability of using the green channel, we also measured the magenta channel and the total intensity using Adobe Photoshop CC v. 19.1.1 (Adobe Systems Incorporated, CA, USA). Both the magenta channel and total intensity correlated with the intensity of green channel (Pearson's correlation, Magenta: $p<.001$, df=17, $R^2=1$; Total intensity: $p<.001$, df=17, $R^2=0.99$).

Malpighian tubule measurement

At the end of the assay, the tubule was photographed to measure its diameter (µm). The length (mm) of the tubule in contact with the treatment solution, was measured by cutting off the two extremities of the tubule outside the bath, laying the remaining section of tubule flat on the Sylgard® base, and photographing it. The surface (mm^2) of the tubule in contact with the bath, was calculated from the cylinder formula:

$$S = 2\pi \left(\frac{d}{2}\right) l$$

where S is the tubule surface, d is the tubule diameter, and l is the tubule length.

Statistical Analysis

All the statistical analysis was conducted in R version 3.4.1 (R Core Team, 2018). We performed Linear Mixed Effect Models (LMEM) with the maximum likelihood estimation by

214 using the `lmer` function from the 'lme4' package (Bates *et al.*, 2014). We performed ANOVA
215 Type II Wald chi-square tests by using the `Anova` function from the 'car' package (Fox and
216 Weisberg, 2012). We used the Akaike information criterion (AIC) (Akaike, 1987) for model
217 selection.

218 To investigate the effect of the treatments on the fluid secretion rate and the net
219 extrusion of rhodamine B, we analysed the interaction between the treatment (categorical)
220 and the surface area (continuous (mm^2)) at each level of time (Table 3,7). For the rhodamine
221 B concentration, we analysed the interaction between treatment (categorical) and secretion
222 rate (continuous (nL/min)) at each time interval (Table 5). To account for the nested structure
223 of data, we included the individual locust as random intercept in the model.

224 To investigate the effect of the incubation time on the fluid secretion rate and the net
225 extrusion of Rhodamine B, we analysed the interaction of the variables time, surface area,
226 and treatment (Table 2,6), whereas for the rhodamine B concentration we analysed the
227 interaction of the variables time, secretion rate, and treatment (Table 4). Again, to account for
228 the nested structure of data, we included the individual locust as random intercept in the
229 model. We also included tubule identity as a random intercept and time as random slope to
230 account for the repeated measurements on the same individual tubule.

231 To investigate the effect of the fluid secretion rate on the net extrusion of Rhodamine
232 B we analysed the interaction of the variables secretion rate and treatment, including as before
233 the individual locust as random intercept (Table 8).

234 To simplify the interpretation of the regression estimates, we centred the surface
235 variable on 2 mm^2. Therefore, all the estimates and comparisons are referred to a tubule with
236 a surface area of 2 mm^2. The models were tested using type II Wald chi-square tests and the
237 non-significant interactions ($P>0.05$) were removed. However, we retained all the main effects
238 even if they were not statistically significant to avoid an increase in the type I error rate
239 (Forstmeier and Schielzeth, 2011).

240 RESULTS

241 We prepared three Malpighian tubules from each locust (see Materials and Methods; Figure
242 1). Each tubule was punctured near the proximal end to allow the luminal fluid to be secreted
243 (Figure 2A), and the first droplet secreted immediately after puncturing discarded. The tubules
244 were then bathed in saline for 30 minutes and the droplet secreted at the end of this period
245 was removed (Figure 2B, Figure 3). The saline was then replaced with one of four treatments:
246 saline (control); rhodamine B 60 μM (R60); rhodamine B 60 μM + verapamil 125 μM (V125);
247 and rhodamine B 60 μM + verapamil 250 μM (V250). Six locusts were used for each of the
248 treatments except for the R60 treatment in which eight locusts were used. Every 30 minutes
249 the droplet secreted by the tubule during the Ramsay assay was removed.

250

251 **Fluid secretion rate and surface area**

252 We determined the fluid secretion rate of each tubule from the volume of the droplet secreted
253 after each 30 minute interval up to 90 minutes after the start of the treatment. Thus, for each
254 tubule we had a measure of the secretion rate in saline during preincubation, and three
255 measurements of the secretion rate in each of the four treatments. In total, there were 76
256 preincubation observations and 233 treatment observations (two droplets were lost during
257 preincubation and another at 60 minutes for the V250 treatment) from 78 Malpighian tubules.

258 To determine whether the surface area of the Malpighian tubules exposed to the bath
259 solution influences the fluid secretion rate, we measured the length and diameter of each
260 tubule immersed in the saline or treatment. By comparing linear mixed effect models that
261 incorporated these measurements of length, diameter or surface area, we determined that
262 surface area was the best explanatory variable (Table 1). There was no difference in the
263 surface area of Malpighian tubules exposed to the bathing solution among the treatments
264 (ANOVA type II Wald, χ^2 =1.72, df=3, P=0.633; Control: 2.00 ± 0.09 mm^2; R60: 2.01 ± 0.06
265 mm^2; V125: 2.27 ± 0.06 mm^2; V250: 2.29 ± 0.07 mm^2).

266 The surface area of the tubule exposed in the bathing solution influenced the fluid
267 secretion rate (ANOVA type II Wald, χ^2 = 47.44, df=1, p<0.001; Table 2, Figure 4). During
268 preincubation the surface area correlated positively with the fluid secretion rate (ANOVA type
269 II Wald, χ^2 = 35.02, df=1, p<.001; Table 3A, Figure 4A). Again, after 30 and 60 minutes of
270 incubation the surface area positively influenced the fluid secretion rate and there was no
271 interaction between surface area and treatment (ANOVA type II Wald, Time 30: χ^2 = 3.19,
272 df=3, p=0.364; Time 60: χ^2 = 2.56, df=3, p=0.465; Table 3A, Figure 4B,C). However, after 90
273 minutes of incubation there was an interaction between surface area and treatment(ANOVA
274 type II Wald, χ^2 = 10.73, df=3, p=0.013; Table 3A, Figure 4D); the R60 and V125 treatment
275 tubules showed a positive correlation between surface area and fluid secretion rate, whereas
276 the V250 treatment tubules showed no significant correlation (Table 3A, Figure 4D).

277 Having incorporated tubule surface area into our statistical model, we were able to
278 compare the fluid secretion rates of our control and treatments objectively. Irrespective of the
279 treatment, the fluid secretion rate decreased significantly in comparison to the secretion rate
280 during preincubation as the experiment progressed (ANOVA type II Wald, χ^2 =283.94, df=3,
281 p<0.001; Table 2, Figure 5). On average, the secretion rate after 90 minutes dropped by 55%
282 in the R60 treatment, by 65% in the control treatment, by 64% in the V125 treatment, and by
283 80% in the V250 treatment (Table 9). Moreover, there was a significant interaction between
284 treatment and time in our statistical model (ANOVA type II Wald, χ^2 =23.81, df=9, p=0.005;
285 Table 2), indicating that although fluid secretion rate decreased with the time of incubation for
286 all treatments, the rate at which it changed depended upon the treatment. Specifically, in

287 comparison to the preincubation baseline, the V250 and the control treatments showed a
288 significantly more pronounced decrease in the secretion rate compared to the R60 treatment,
289 whereas the V125 treatment did not differ from the R60 treatment (Table 2, Figure 5).
290 However, when comparing the fluid secretion rate between treatments at each time point,
291 there was no significant difference between the R60 tubules' secretion rates and those of the
292 three other treatments (Table 3B, Figure 5).
293
294 **Net extrusion of Rhodamine B**
295 We determined the concentration of Rhodamine B in each of the droplets collected from the
296 Malpighian tubules exposed to the R60, V125 and V250 treatments at each time point. The
297 concentration of rhodamine B in the droplets increased significantly during the incubation time
298 in all the treatments (ANOVA type II Wald, χ^2 = 259.29, df=2, p<.001; Table 4, Figure 6). There
299 was a significant interaction between treatment and time (ANOVA type II Wald, χ^2 =85.32,
300 df=4, p<.001; Table 4, Figure 6), indicating that the increase in the rhodamine B concentration
301 over time depended upon the treatment. In particular, the increase in rhodamine B
302 concentration in the R60 treatment was more pronounced than in either the V125 or V250
303 treatments (Table 4, Figure 6). At each time point, the treatment significantly affected the
304 rhodamine B concentration (ANOVA type II Wald, Time 30: χ^2=58.17, df=2, p<.001; Time 60:
305 χ^2=81.86, df=2, p<.001; Time 90: χ^2=89.27, df=2, p<.001; Table 5, Figure 6). Compared to the
306 R60 treatment, the addition of verapamil in the V125 and V250 treatments reduced the
307 rhodamine B concentration of the secreted droplets after 30, 60, and 90 minutes (Table 5,
308 Figure 6). However, there was no significant difference in the rhodamine B concentration
309 between the V125 and V250 treatments at any time point (Table 5, Figure 6).
310 We calculated the total number of moles of rhodamine B extruded by the Malpighian
311 tubules per minute as the product of the secretion rate and the rhodamine B concentration of
312 the droplets secreted, which we termed the net extrusion rate. The net extrusion increased
313 significantly during the incubation time (ANOVA type II Wald, χ^2 = 153.2, df=2, p<.001; Table
314 6, Figure 7). At each time point, treatment affected the net extrusion of rhodamine B (ANOVA
315 type II Wald, time 30: χ^2=23.97, df=2, p<.001; time 60: χ^2=23.69, df=2, p<.001; time 90: χ^2
316 =28.75, df=2, p<.001; Table 7A, Figure 7A). In comparison to the R60 treatment, the addition
317 of verapamil in the V125 and V250 treatments significantly reduced the net extrusion of
318 rhodamine B after 30, 60 and 90 minutes, however, there was no significant difference
319 between the V125 and V250 treatments (Table 7A, Figure 7A).
320 There was also an interaction between treatment, time and surface (ANOVA type II
321 Wald, χ^2 = 11.36, df=4, p=.023; Table 6, Figure 8), indicating that the dependency of the net
322 extrusion of rhodamine B upon tubule surface area was influenced by the incubation time and
323 the treatment (Table 6, Figure 8). There was no interaction between surface and treatment

after 30 minutes (ANOVA type II Wald, time 30: χ^2 =3.36, df=2, p=.186; Table 7B, Figure 8A). However, after 60 and 90 minutes the effect of surface area upon the net extrusion of rhodamine B was more pronounced in the R60 treatment than in the V125 and V250 treatments (ANOVA type II Wald, time 60: χ^2 =8.94, df=2, p=.011; time 90: χ^2 =17.54, df=2, p<.001; Table 7B, Figure 8B,C).

In addition, we found that after 30 minutes the fluid secretion rate of the tubules incubated in R60 positively influenced the net extrusion of rhodamine B, while there was no significant effect in the V125 and V250 treatments (ANOVA type II Wald, treatment x fluid secretion rate, time 30: χ^2 =72.26, df=2, p<.001; Table 8, Figure 9A). After 60 and 90 minutes, the fluid secretion rate positively correlated with the net extrusion of rhodamine B in all the treatments (Table 8, Figure 9B,C). However, the surface area of the tubules incubated in R60 showed a more pronounced effect on the net extrusion of rhodamine B than that of the tubules incubated in V125 and V250 (ANOVA type II Wald, treatment x fluid secretion rate, time 60: χ^2 =101.04, df=2, p<.001; time 90: χ^2 =30.13, df=2, p<.001; Table 8, Figure 9).

Net contribution of P-glycoproteins

A single Malpighian tubule with a mean surface of 2 mm^2 incubated in a solution of 60 µM rhodamine B, extruded rhodamine B with a rate of 18.8 ± 2.6 fmol/min in the first 30 minutes, 54.7 ± 7.3 fmol/min between 30 and 60 minutes and 80.3 ± 9.3 fmol/min between 60 and 90 minutes (Table 9). The addition of verapamil significantly reduced the amount of rhodamine B extruded, but did not block it completely (Table 9, Table 7). The rhodamine B concentration of the droplets secreted did not differ between the V125 and V250 treatments (Table 5, Table 9). Therefore, we assumed that 125 µM verapamil was sufficient to inhibit all the P-glycoproteins that are verapamil sensitive and that passive diffusion and other types of pumps may contribute to extrusion of Rhodamine B. Consequently, we subtracted the mean values of the net extrusion of rhodamine B obtained from the V250 treatment from the net extrusion of the R60 treatment to estimate the contribution of the P-glycoproteins alone. The average rates of rhodamine B extruded by the P-glycoproteins were 17.2 fmol/min, 43.4 fmol/min and 59.1 fmol/min between 0-30, 30-60 and 60-90 minutes respectively (Table 9, Figure 7B, dashed line). In percentage, the P-glycoproteins are responsible for the 91%, 79% and 74% (between 0-30, 30-60 and 60-90 minutes respectively) of the total extrusion of rhodamine B. Overall, P-glycoproteins account for the 78% of the total extrusion of rhodamine B, over the 90 minutes of incubation.

DISCUSSION

359 Our aim was to determine whether P-glycoprotein transporters are involved in the removal of
360 xenobiotic substances by Malpighian tubules from the haemolymph of desert locusts and, if
361 so, how they perform physiologically. To this end, we developed an alternative method to liquid
362 chromatography–mass spectrometry (Andersson *et al*., 2013), radiolabelled alkaloids
363 (Gaertner *et al*., 1998) or confocal microscopy (Leader and O'Donnell, 2005; O'Donnell and
364 Leader, 2006) based upon measuring dye concentration. A similar method has been used
365 previously to investigate epithelial transport in tardigrades and desert locusts using
366 chlorophenol red by imagining through the gut or tubules (Halberg and Møbjerg, 2012). By
367 imaging extruded drops from Malpighian tubules, we assessed the performance of epithelial
368 transporters more accurately than by imaging the lumen of the tubules. We used the P-
369 glycoprotein substrate rhodamine B (Eytan *et al*., 1997) and the P-glycoprotein inhibitor
370 verapamil (Tsuruo *et al*., 1981) to assay P-glycoprotein function through the colour of the
371 droplets secreted by the Malpighian tubules. Using this strategy, we obtained evidence that
372 desert locust Malpighian tubules express a P-glycoprotein transporter, that the fluid secretion
373 rate of these tubules is proportional to their surface area, and that the fluid secretion rate
374 influences the net extrusion of rhodamine B.
375
376 **A P-glycoprotein transporter extrudes xenobiotics in desert locust Malpighian tubules**
377 Our conclusion that desert locust Malpighian tubules express P-glycoproteins is supported by
378 two lines of evidence. Firstly, these tubules actively extrude the dye rhodamine B, a P-
379 glycoprotein substrate (e.g. Eytan *et al*., 1997; Mayer *et al*., 2009), when it is present in the
380 solution in which they are bathed. Rhodamine B has been widely used as a substrate for P-
381 glycoproteins in cell culture and blood brain barrier models (e.g. Eytan *et al*., 1997; Mayer *et*
382 *al*., 2009). Secondly, the addition of verapamil, a P-glycoprotein inhibitor (e.g. Andersson *et*
383 *al*., 2014; Dermauw and Van Leeuwen, 2014; Hamada *et al*., 1987; Tsuruo *et al*., 1981),
384 significantly reduced the extrusion of rhodamine B. The presence of P-glycoproteins in other
385 tissues of the desert locusts also supports our conclusion that they are expressed in the
386 Malpighian tubules; proteins with a comparable physiology and similar sequence to the human
387 P-glycoprotein (ABCB1 gene) are expressed within the blood brain barrier of the locusts *S.*
388 *gregaria* and *L. migratoria* (Al-Qadi *et al*., 2015; Andersson *et al*., 2014, 2013; Nielsen *et al*.,
389 2011). Further support comes from comparison with other insects; P-glycoprotein transporters
390 have been found in the Malpighian tubules of many other insects including the black field
391 cricket (*Teleogryllus commodus*; Leader and O'Donnell, 2005), tobacco hornworm (*Manduca*
392 *sexta*; Gaertner *et al*., 1998; Murray *et al*., 1994), fruit fly (*D. melanogaster*), kissing bug
393 (*Rhodnius prolixus*), large milkweed bug (*Oncopeltus fasciatus*), yellow fever mosquito (*Aedes*
394 *aegypti*), house cricket (*Acheta domesticus*), migratory locust (*Locusta migratoria*), mealworm

395 beetle (*Tenebrio molitor*), and the American cockroach (*Periplaneta americana*; Rheault *et al.*,
396 2006).
397 Rhodamine B extrusion was not blocked entirely by 125 μM verapamil or by double
398 this concentration. Comparison of the extent of the reduction at both concentrations suggests
399 that even at the lower verapamil concentration all the P-glycoproteins were inhibited. This
400 suggests that approximately 78% of rhodamine B was transported by P-glycoproteins via a
401 verapamil sensitive mechanism, whilst the remaining 22% was verapamil insensitive.
402 Moreover, after 90 minutes the concentration of rhodamine B in the droplets secreted by the
403 Malpighian tubules was higher than that of the bathing solution suggesting that rhodamine B
404 transport in the presence of verapamil is not simply due to passive diffusion, but that other
405 active transporters may be implicated. Several potential candidates for alternative active
406 transporters exist. For example, in human cell lines (Calu-3), rhodamine B can interact with
407 multiple organic cation transporters (OCT3, OCTN1,2) (Ugwu *et al.*, 2016). Potentially,
408 however, verapamil may be incapable of blocking rhodamine B transport completely allowing
409 a small number of rhodamine B molecules to be extruded by the P-glycoprotein even in the
410 presence of verapamil.
411 Verapamil inhibits P-glycoproteins and does not interact with other multidrug
412 resistance proteins (Cole *et al.*, 1989). This suggests that the effects of verapamil in our
413 experiments are through its specific effects upon P-glycoproteins. The mechanistic basis of
414 verapamil inhibition is unclear but the most widely accepted explanation is that P-glycoproteins
415 extrude both verapamil and their substrate but that verapamil diffuses back across the lipid
416 bilayer much faster than the substrate creating a futile cycle and thereby competing with the
417 substrate transport (Eytan *et al.*, 1996; for a review see Sharom, 1997).
418 Verapamil is, however, also a known L-type Ca^{2+} channel blocker (Abernethy and
419 Schwartz, 1999). In *Drosophila*, L-type Ca^{2+} channels are expressed in the basolateral and
420 apical membranes of the tubule principal cells, and are involved in the regulation of the fluid
421 secretion (MacPherson *et al.*, 2001). Indeed, an increase of the intracellular Ca^{2+} level
422 mediates the effect of diuretic hormones (Paluzzi *et al.*, 2013). Verapamil reduced the fluid
423 secretion of *Drosophila* Malpighian tubules stimulated by peptide agonists (e.g. CAP2b,
424 cGMP) but had no effect on unstimulated tubules (MacPherson *et al.*, 2001). Our experiments
425 cannot exclude the possibility that verapamil affects Ca^{2+} channels in locust Malpighian
426 tubules by interfering with intracellular Ca^{2+}, and thereby has an indirect effect on Rhodamine
427 B extrusion. Because the fluid secretion rate did not differ between treatments, however, the
428 reduction in the net extrusion of rhodamine B was likely caused solely by verapamil inhibition
429 of the P-glycoproteins. Thus, when considered within the context of the expression of P-
430 glycoproteins in the blood brain barrier of locusts (Al-Qadi *et al.*, 2015; Andersson *et al.*, 2014,
431 2013; Nielsen *et al.*, 2011) and the expression of P-glycoproteins in homologous Malpighian

432 tubules in other insects species (see above), it seems highly likely that the tubules of
433 gregarious desert locust express P-glycoproteins.
434
435 **Malpighian tubule surface area and fluid secretion rate**
436 We used linear mixed effect models to determine which physical feature of a tubule, its surface
437 area, length or diameter has the greatest influence on fluid secretion rate. We found that the
438 surface area of the Malpighian tubules positively influences their fluid secretion rate, and more
439 accurately predicts the fluid secretion rate than tubule diameter or length. Some previous
440 studies have reported that tubule length was linearly related to the fluid secretion rate
441 (Beyenbach *et al*., 1993; Coast, 1988) but in our analysis length was a consistently worse than
442 surface area as a predictor. Even when the surface area (or length) has been accounted for
443 in previous studies, this has involved dividing the fluid secretion rate by the surface area (or
444 length) to obtain the fluid secretion rate per unit area (or unit length) (Bradley, 1983; Rheault
445 *et al*., 2006). Although this approach is useful when comparing tubules of different sizes from
446 different insect species, it fails to reveal the exact relationship between the surface area and
447 the fluid secretion rate. Our statistical models demonstrate that interactions between factors
448 such as surface area and fluid secretion rate depend upon the treatment applied, and are not
449 static changing over time with treatment. For example, our results show that the fluid secretion
450 rate increases with the increasing of the tubule surface apart from after 90 minutes of
451 incubation with 250 μM verapamil, where the surface no longer influences the fluid secretion
452 rate. Such interdependencies are unlikely to be detected or accounted for in simpler statistical
453 analyses, causing such interdependencies to be ignored.
454
455 **Determining the transepithelial transport of xenobiotics by P-glycoprotein transporters**
456 **in locust Malpighian tubules**
457 Transepithelial transport of xenobiotics by P-glycoproteins across the inner membrane of the
458 Malpighian tubules can be determined from the net extrusion rate we measured. The disparity
459 between the transepithelial transport and the net extrusion rate is due to the properties of
460 rhodamine B. This lipophilic dye can passively permeate the lipid bilayer of liposomes,
461 following the concentration gradient (Eytan *et al*., 1997). Likewise, in desert locust Malpighian
462 tubules, rhodamine B can back diffuse into the bath solution when active transporters increase
463 its luminal concentration creating a concentration gradient. Consequently, the fluid secretion
464 rate affects the net extrusion rate of rhodamine B because a decrease in the fluid secretion
465 will increase the luminal concentration of the dye, allowing greater back diffusion whilst an
466 increase in the fluid secretion rate will have the opposite effect (Maddrell *et al*., 1974).
467 Therefore, if a dye, like rhodamine B, can back diffuse, its net extrusion will be proportional to

468 the fluid secretion rate (Supplemental Figure 3A-C), while if the dye cannot back diffuse there
469 will be no correlation (Supplemental Figure 3D-F). When the rhodamine B concentration in the
470 lumen was lower or similar to the bath (60 μM) the net transport would be little affected by the
471 secretion rate. Conversely, when the luminal rhodamine B concentration was higher than the
472 bathing solution, part of the dye diffused back, so that the net extrusion was significantly
473 influenced by the fluid secretion rate (see supplementary material).
474 Previous studies demonstrated that Malpighian tubules can exhibit different degrees
475 of passive permeability to different substances, depending on the species and on the
476 properties (i.e. size, polarity) of the substrate used (e.g. dyes, alkaloid, drugs) (Maddrell *et al*.,
477 1974). For example, tubules of the kissing bug (*R. prolixus*) have passive permeability to the
478 alkaloid nicotine (Maddrell and Gardiner, 1976), but not to the dye indigo carmine (Maddrell *et*
479 *al.*, 1974), whereas tubules of the blowfly (*Calliphora erythrocephala*) are permeable to indigo
480 carmine (Maddrell *et al.,* 1974). Thus, when studying the effect of a substance on active
481 transporters, it is important to take into account the fluid secretion rate because a change in
482 the net extrusion rate of a substrate may be caused not only by a direct effect on the
483 transporters, but also by an indirect consequence of a change in the fluid flow (O'Donnell and
484 Leader, 2006). In our experiment, the fluid secretion rate did not differ between treatments,
485 indicating that the reduction of net extrusion of rhodamine B following exposure to verapamil
486 was caused solely by inhibition of the P-glycoprotein. However, the fluid secretion rate
487 decreased over time, which may produce an underestimation of the net transepithelial
488 transport of rhodamine B.
489
490 **Implications for desert locust detoxification**
491 Gregarious desert locusts feed on a broad variety of plants including species containing
492 secondary metabolites such as atropine to become unpalatable to predators (Despland and
493 Simpson, 2005; Mainguet *et al*., 2000; Sword *et al*., 2000; for a review see Pener and Simpson,
494 2009). The expression of P-glycoproteins in the Malpighian tubules to extrude noxious
495 substances may be an adaptation to cope with the ingestion of toxic plants. This may also be
496 the reason for expression of P-glycoproteins on the blood brain barrier of desert locusts, which
497 would prevent the uptake of hydrophobic substances in the central nervous system
498 (Andersson *et al*., 2014). Yet the relationship between ingesting toxins and detoxification
499 pathways in the Malpighian tubules is not straightforward; some species of Orthoptera, as well
500 as Coleoptera, Lepidoptera, Heteroptera, Hymenoptera and Sternorrhyncha (for a review see
501 Opitz and Müller, 2009), sequester toxins from the plants they ingest to deter predators.
502 However, toxicity may also be conferred by gut contents, rather than through sequestration
503 within bodily tissues. For example, the chemical defence of the spotted bird grasshopper,
504 *Schistocerca emarginata* (=*lineata*), is mediated by the contents of toxic plant in its gut (Sword,

505 2001, 1999). This species is a congener of the desert locust, *S. gregaria*, which suggests that
506 a similar strategy may be involved in the production of toxicity in this species. If this is the
507 case, then the presence of toxins in the haemolymph may be a consequence of ingesting toxic
508 plant material for storage within the gut. In such a scenario, detoxification pathways within the
509 Malpighian tubules would then be essential for ensuring that toxins do not accumulate within
510 the haemolymph to concentrations that would affect physiological processes.
511 The P-glycoprotein detoxification pathway that we have characterised in desert locusts
512 is likely to be highly effective in extruding xenobiotic compounds from haemolymph, especially
513 when the number of Malpighian tubules within an individual locust is considered. However, it
514 is important to consider that the locusts used for our experiments have experienced a diet free
515 of toxins, such as atropine. P-glycoprotein expression can be modulated depending on the
516 diet (Tapadia and Lakhotia, 2005); *Drosophila* larvae fed on colchicine increased the
517 expression of the P-glycoprotein gene homologue mdr49 in the brain and gut. Consequently,
518 adult gregarious desert locusts that have fed on a diet including plant toxins may have even
519 stronger P-glycoprotein detoxification pathways. In contrast to their gregarious counterparts,
520 solitary desert locusts actively avoid plants containing atropine (Despland and Simpson,
521 2005), and find odours associated with it aversive (Simões *et al.*, 2013). Thus, Malpighian
522 tubules of solitary desert locusts may express fewer P-glycoproteins than those of the
523 gregarious phase, possibly due to their reduced exposure to secondary metabolites from their
524 diet.
525
526 **Implications for insect pest control**
527 P-glycoproteins are implicated in the resistance of some insect pests to insecticides (Lanning
528 *et al.*, 1996) promoting the efflux of various xenobiotics thereby decreasing the intracellular
529 drug accumulation. For instance, P-glycoproteins have been detected in a resistant strain of
530 the pest cotton bollworm (*Helicoverpa armigera*) but not in a susceptible one (Srinivas *et al.*,
531 2004). P-glycoproteins have also been implicated in the protection of the mitochondria from
532 insecticide damage (Akbar *et al.*, 2014). In Africa and Asia, applications of insecticides are
533 carried out (Van Huis, 2007) to try to control desert locust plagues. To increase the efficacy,
534 a combination of P-glycoprotein inhibitors and insecticide may act synergistically to increase
535 the locust mortality, reducing the amount of insecticide used. Further investigation into the
536 interaction between P-glycoproteins and different xenobiotics (i.e. insecticides, herbicides,
537 miticides and secondary metabolites) may improve our understanding of the physiological
538 effect of pesticides on insects, and subsequently lead to the development of more specific
539 targeted insecticides.
540
541 **Acknowledgements**

542 M.R. was financially supported by a graduate studentship from the School of Life Sciences,
543 University of Sussex. D.D.B was financially supported by the Welsh government/HEFCW
544 RESILCOAST project.

545

546 **Authors' contributions**

547 M.R. and J.E.N conceived the experiment; M.R. and J.E.N designed the experiments. M.R.
548 carried out the experiments, analysed the images and carried out the data analyses. D.D.B
549 provided help for the statistical analyses. M.R. and J.E.N wrote the manuscript.

550

551 ## References

552 Abernethy, D.R. and Schwartz, J.B. (1999). Calcium-antagonist drugs. *New England J.*
553 *Medicine*, *341*, 1447-1457.

554 Akaike, H. (1987). Factor analysis and AIC. *In Selected papers of Hirotugu Akaike* (pp. 371-
555 386). Springer, New York, NY.

556 Akbar, S.M., Aurade, R.M., Sharma, H.C. and Sreeramulu, K. (2014). Mitochondrial P-
557 glycoprotein ATPase contributes to insecticide resistance in the cotton bollworm,
558 *Helicoverpa armigera* (Noctuidae: Lepidoptera). *Cell Biochem. Biophys.*, *70*, 651-660.

559 Al-Qadi, S., Schiøtt, M., Hansen, S.H., Nielsen, P.A. and Badolo, L. (2015). An invertebrate
560 model for CNS drug discovery: Transcriptomic and functional analysis of a mammalian P-
561 glycoprotein ortholog. *Biochimica Biophysica Acta*, *1850*, 2439-2451.

562 Andersson, O., Badisco, L., Hansen, A.H., Hansen, S.H., Hellman, K., Nielsen, P.A., Olsen,
563 L.R., Verdonck, R., Abbott, N.J., Vanden Broeck, J. and Andersson, G. (2014).
564 Characterization of a novel brain barrier *ex vivo* insect-based P-glycoprotein screening
565 model. *Pharmacol. Res. Perspectives*, *2*, e00050

566 Andersson, O., Hansen, S.H., Hellman, K., Olsen, L.R., Andersson, G., Badolo, L.,
567 Svenstrup, N. and Nielsen, P.A. (2013). The grasshopper: a novel model for assessing
568 vertebrate brain uptake. *J. Pharmacol. Exper. Therapeut.*, *346*, 211-218.

569 Bates, D., Mächler, M., Bolker, B. and Walker, S. (2014). Fitting linear mixed-effects models
570 using lme4. *arXiv preprint arXiv:1406.5823.*

571 Beyenbach, K.W., Oviedo, A. and Aneshansley, D.J. (1993). Malpighian tubules of *Aedes*
572 *aegypti:* five tubules, one function. *J Ins. Phys.*, *39*(8), 639-648.

573 Bradley, T.J. (1983). Functional design of microvilli in the Malpighian tubules of the insect
574 *Rhodnius prolixus*. *J. Cell Sci.*, *60*, 117-135.

575 Coast, G.M. (1988). Fluid secretion by single isolated Malpighian tubules of the house
576 cricket, Acheta domesticus, and their response to diuretic hormone. *Phys. Entom., 13*(4),
577 381-391.

578 Cole, S.P.C., Downes, H.F. and Slovak, M.L. (1989). Effect of calcium antagonists on the
579 chemosensitivity of two multidrug-resistant human tumour cell lines which do not
580 overexpress P-glycoprotein. *Brit. J. Cancer*, *59*, 42.

581 Dermauw, W. and Van Leeuwen, T. (2014). The ABC gene family in arthropods:
582 comparative genomics and role in insecticide transport and resistance. *Insect Biochem. Mol.*
583 *Biology*, *45*, 89-110.

584 Despland, E. and Simpson, S.J. (2005). Food choices of solitarious and gregarious locusts
585 reflect cryptic and aposematic antipredator strategies. *Anim. Behav.*, *69*, 471-479.

586 Eytan, G.D., Regev, R., Oren, G. and Assaraf, Y.G. (1996). The role of passive transbilayer
587 drug movement in multidrug resistance and its modulation. *J. Biological Chem.*, *271*, 12897-
588 12902.

589 Eytan, G.D., Regev, R., Oren, G., Hurwitz, C.D. and Assaraf, Y.G. (1997). Efficiency of P-
590 glycoprotein–mediated exclusion of rhodamine dyes from multidrug-resistant cells is
591 determined by their passive transmembrane movement rate. *Eur. J. Biochem.*, *248*, 104-
592 112.

593 Forstmeier, W. and Schielzeth, H. (2011). Cryptic multiple hypotheses testing in linear
594 models: overestimated effect sizes and the winner's curse. *Behav. Ecol. Sociobiol.*, *65*, 47-
595 55.

596 Fox, J., Weisberg, S., Adler, D., Bates, D., Baud-Bovy, G., Ellison, S., Firth, D., Friendly, M.,
597 Gorjanc, G., Graves, S. and Heiberger, R. (2012). Package 'car'. *Vienna: R Found. Stat.*
598 *Comp.*

599 Gaertner, L.S., Murray, C.L. and Morris, C.E. (1998). Transepithelial transport of nicotine
600 and vinblastine in isolated malpighian tubules of the tobacco hornworm (*Manduca sexta*)
601 suggests a P-glycoprotein-like mechanism. *J. Exp. Biol.*, *201*, 2637-2645.

602 Guseman, A.J., Miller, K., Kunkle, G., Dively, G.P., Pettis, J.S., Evans, J.D. and Hawthorne,
603 D.J. (2016). Multi-drug resistance transporters and a mechanism-based strategy for
604 assessing risks of pesticide combinations to honey bees. *PLoS ONE*, *11*, e0148242.

605 Halberg, K.A. and Møbjerg, N. (2012). First evidence of epithelial transport in tardigrades: a
606 comparative investigation of organic anion transport. *J. Exp. Biol.*, *215*, 497-507.

607 Hawthorne, D.J. and Dively, G.P. (2011). Killing them with kindness? In-hive medications
608 may inhibit xenobiotic efflux transporters and endanger honey bees. *PloS One*, *6*, e26796.

609 Hamada, H., Hagiwara, K.I., Nakajima, T. and Tsuruo, T. (1987). Phosphorylation of the Mr
610 170,000 to 180,000 glycoprotein specific to multidrug-resistant tumor cells: effects of
611 verapamil, trifluoperazine, and phorbol esters. *Cancer Research*, *47*, 2860-2865.

612 Karnaky Jr, K.J., Petzel, D., Sedmerova, M., Gross, A. and Miller, D.S. (2000). Mrp2-like
613 transport of Texas Red by Malpighian tubules of the common American cockroach,
614 *Periplaneta americana*. *Bull. Mt. Des. Isl. Biol. Lab*, *39*, 52-53.

615 Lanning, C.L., Fine, R.L., Corcoran, J.J., Ayad, H.M., Rose, R.L. and Abou-Donia, M.B.
616 (1996). Tobacco budworm P-glycoprotein: biochemical characterization and its involvement
617 in pesticide resistance. *Biochimica Biophysica Acta*, *1291*, 155-162.

618 Leader, J.P. and O'Donnell, M.J. (2005). Transepithelial transport of fluorescent p-
619 glycoprotein and MRP2 substrates by insect Malpighian tubules: confocal microscopic
620 analysis of secreted fluid droplets. *J. Exp. Biol.*, *208*, 4363-4376.

621 MacPherson, M.R., Pollock, V.P., Broderick, K.E., Kean, L., O'Connell, F.C., Dow, J.A. and
622 Davies, S.A. (2001). Model organisms: new insights into ion channel and transporter

623 function. L-type calcium channels regulate epithelial fluid transport in *Drosophila*
624 *melanogaster. Am. J. Physiol. Cell Physiol.*, *280*, C394-407.

625 Maddrell, S.H. and Gardiner, B.O. (1976). Excretion of alkaloids by Malpighian tubules of
626 insects. *J. Exp. Biol.*, *64*, 267-281.

627 Maddrell, S.H.P., Gardiner, B.O.C., Pilcher, D.E.M. and Reynolds, S.E. (1974). Active
628 transport by insect Malpighian tubules of acidic dyes and of acylamides. *J. Exp. Biol.*, *61*,
629 357-377.

630 Maddrell, S.H.P. and Klunsuwan, S. (1973). Fluid secretion by in vitro preparations of the
631 Malpighian tubules of the desert locust *Schistocerca gregaria*. *J. Ins. Phys.*, *19*, 1369-1376.

632 Mainguet, A.M., Louveaux, A., El Sayed, G. and Rollin, P. (2000). Ability of a generalist
633 insect, *Schistocerca gregaria*, to overcome thioglucoside defense in desert plants: tolerance
634 or adaptation? *Entom. Experim. App.*, *94*, 309-317.

635 Mayer, F., Mayer, N., Chinn, L., Pinsonneault, R.L., Kroetz, D. and Bainton, R.J. (2009).
636 Evolutionary conservation of vertebrate blood–brain barrier chemoprotective mechanisms in
637 *Drosophila*. *J. Neurosci.*, *29*, 3538-3550.

638 Murray, C.L., Quaglia, M., Arnason, J.T. and Morris, C.E. (1994). A putative nicotine pump at
639 the metabolic blood–brain barrier of the tobacco hornworm. *J. Neurobiol.*, *25*, 23-34.

640 Nielsen, P.A., Andersson, O., Hansen, S.H., Simonsen, K.B. and Andersson, G. (2011).
641 Models for predicting blood–brain barrier permeation. *Drug Disc. Today*, *16*, 472-475.

642 O'Donnell, M.J. (2008). Insect excretory mechanisms. *Adv. Ins. Phys.*, *35*, 1-122.

643 O'Donnell, M.J. and Leader, J.P. (2006). Changes in fluid secretion rate alter net
644 transepithelial transport of MRP2 and P-glycoprotein substrates in Malpighian tubules of
645 *Drosophila melanogaster*. *Arch. Ins. Biochem. Phys.*, *63*, 123-134.

646 Opitz, S.E. and Müller, C. (2009). Plant chemistry and insect sequestration. *Chemoecol.*, *19*,
647 117.

648 Paluzzi, J.P., Yeung, C. and O'Donnell, M.J. (2013). Investigations of the signaling cascade
649 involved in diuretic hormone stimulation of Malpighian tubule fluid secretion in *Rhodnius*
650 *prolixus*. *J Ins. Phys.*, *59*(12), 1179-1185.

651 Pener, M.P. and Simpson, S.J. (2009). Locust phase polyphenism: an update. *Adv. Insect*
652 *Physiol.*, *36*, 1-272.

653 Phillips, J.E. (1964). Rectal absorption in the desert locust, *Schistocerca gregaria* Forskal.
654 I. *J. Exp. Biol*, *41*, 15-38.

655 Ramsay, J.A. (1954). Active transport of water by the Malpighian tubules of the stick insect,
656 *Dixippus morosus* (Orthoptera, Phasmidae). *J. Exp. Biol.*, *31*, 104-113.

657 Ramsay, J.A. (1958). Excretion by the Malpighian tubules of the stick insect, *Dixippus*
658 *morosus* (Orthoptera, Phasmidae): amino acids, sugars and urea. *J. Exp. Biol.*, *35*, 871-891.

659 R Core Team (2016). R: A language and environment for statistical computing. R
660 Foundation for Statistical Computing, Vienna, Austria. URL https://www.R-project.org/.

661 Rheault, M.R., Plaumann, J.S. and O'Donnell, M.J. (2006). Tetraethylammonium and
662 nicotine transport by the Malpighian tubules of insects. *J. Insect Physiol.*, *52*, 487-498.

663 Simões, P.M., Niven, J.E. and Ott, S.R. (2013). Phenotypic transformation affects
664 associative learning in the desert locust. *Curr. Biol.*, *23*(23), 2407-2412.

665 Schneider, C.A., Rasband, W.S. and Eliceiri, K.W. (2012). NIH Image to ImageJ: 25 years of
666 image analysis. *Nature methods*, *9*(7), 671.

667 Sharom, F.J. (1997). The P-glycoprotein efflux pump: how does it transport drugs?. *J.*
668 *Memb. Biol.*, *160*, 161-175.

669 Srinivas, R., Udikeri, S.S., Jayalakshmi, S.K. and Sreeramulu, K. (2004). Identification of
670 factors responsible for insecticide resistance in *Helicoverpa armigera*. *Comp. Biochem.*
671 *Phys. Part C: Toxic. Pharm.*, *137*, 261-269.

672 Sword, G.A. (1999). Density-dependent warning coloration. *Nature*, *397*, 217.

673 Sword, G.A. (2001). Tasty on the outside, but toxic in the middle: grasshopper regurgitation
674 and host plant-mediated toxicity to a vertebrate predator. *Oecologia*, *128*, 416-421.

675 Sword, G.A., Simpson, S.J., El Hadi, O.T.M. and Wilps, H. (2000). Density–dependent
676 aposematism in the desert locust. *Proc. R. Soc. B*, *267*, 63-68.

677 Tapadia, M.G. and Lakhotia, S.C. (2005). Expression of mdr49 and mdr65 multidrug
678 resistance genes in larval tissues of *Drosophila melanogaster* under normal and stress
679 conditions. *Cell Stress Chap.*, *10*, 7.

680 Tsuruo, T., Iida, H., Tsukagoshi, S. and Sakurai, Y. (1981). Overcoming of vincristine
681 resistance in P388 leukemia *in vivo* and *in vitro* through enhanced cytotoxicity of vincristine
682 and vinblastine by verapamil. *Canc. Res.*, *41*, 1967-1972.

683 Ugwu, M.C., Oli, A., Esimone, C.O. and Agu, R.U. (2016). Organic cation rhodamines for
684 screening organic cation transporters in early stages of drug development. *J. Pharm. Tox.*
685 *Met.*, *82*, 9-19.

686 Van Huis, A. (2007). Strategies to control the Desert Locust *Schistocerca gregaria*. In *Area-*
687 *Wide Control of Insect Pests* (285-296). Springer, Dordrecht.

688 Wieczorek, H. (1992). The insect V-ATPase, a plasma membrane proton pump energizing
689 secondary active transport: molecular analysis of electrogenic potassium transport in the
690 tobacco hornworm midgut. *J. Exp. Biol.*, *172*, 335-343.

691 Williams, J.C., Hagedorn, H.H. and Beyenbach, K.W. (1983). Dynamic changes in flow rate
692 and composition of urine during the post-bloodmeal diuresis in *Aedes aegypti* (L.). *J. Comp.*
693 *Physiol. B, 153*, 257-265.

694 Wright, S.H. and Dantzler, W.H. (2004). Molecular and cellular physiology of renal organic
695 cation and anion transport. *Physiological Rev.*, *84*, 987-1049.

696

697 **FIGURE LEGENDS**

698 **Figure 1. The extraction and preparation of Malpighian tubules for *ex vivo***
699 **experimentation from the desert locust, *Schistocerca gregaria*.** A) Cutting the posterior
700 tip of the abdomen permits removal of the head and the fully intact gut. B) The gut is
701 submerged in saline and the Malpighian tubules are exposed. The head is separated from the
702 saline bath by a barrier of modelling clay. C) Three tubules are removed from each locust and

703 fixed on a Sylgard® surface traversing a small drop of bathing solution, and covered with
704 paraffin oil.

705 **Figure 2. The experimental scheme for assaying the presence of P-glycoproteins within**
706 **the Malpighian tubules of the desert locust.** A) Individual tubules are severed from the gut
707 and the proximal and distal ends of the tubule are wound around Minuten pins to fix them.
708 Once the saline bath and paraffin oil have been applied, the proximal end of the tubule is
709 punctured with a sharpened capillary tube. B) After 30 minutes of preincubation in saline bath
710 the droplet was removed. C) The saline bath was replaced by a bath containing one of the
711 treatments. D) Every 30 minutes the secreted droplet was removed, placed on the Petri dish
712 and photographed.

713 **Figure 3. Examples of the droplets secreted by the Malpighian tubules of desert locusts**
714 **during preincubation in saline and at every 30 minutes in each of the different**
715 **treatments.** The size of each droplet depends upon the fluid secretion rate whereas the colour
716 is determined by the net extrusion rate of rhodamine B.

717 **Figure 4. Tubule surface area positively influences the fluid secretion rate.** A) A plot of
718 the surface area of the tubule exposed to the bath versus the fluid secretion rate for each of
719 the four treatments during preincubation. B) As in 'A' but 30 minutes after the saline bath was
720 replaced by one of the four treatment baths. C) As in 'B' but after 60 minutes. D) As in 'B' but
721 after 90 minutes. Open circles indicate the fluid secretion rates of individual tubules at a
722 particular time point. Each line with the shaded area around represents the mixed effect model
723 fit with the standard error.

724 **Figure 5. The mean fluid secretion rate of Malpighian decreased with time in all the**
725 **treatments.** A plot of the time from the replacement of the preincubation saline bath with one
726 of the four treatments. Open circles indicate the fluid secretion rates of individual tubules at a
727 particular time point. Each line with the shaded area around represents the mixed effect model
728 fit with the standard error.

729 **Figure 5. The mean rhodamine B concentration of the droplets secreted by the**
730 **Malpighian tubules increased over time in all the treatments.** The addition of verapamil
731 (125 or 250 μM) reduced the rhodamine concentration of the droplets secreted compared with
732 the control treatment 60 μM rhodamine. Open circles indicate the rhodamine concentration of
733 the droplets secreted by individual tubules at a particular time point. Each line with shaded
734 region represents the mixed effect model fit with the standard error.

735 **Figure 6. The mean net extrusion of rhodamine B increased over time in all the**
736 **treatments.** The addition of verapamil (125 or 250 μM) reduced the net extrusion of rhodamine
737 B compared with the control treatment 60 μM Rhodamine. Open circles indicate the net
738 extrusion of rhodamine B by individual tubules at a particular time point. Each line with shaded
739 region represents the mixed effect model fit with the standard error. The dashed line
740 represents the net contribution of the P-glycoproteins obtained by subtracting the net extrusion
741 of rhodamine in the V250 treatment from the R60.

742 **Figure 7. Tubule surface area positively influences the net extrusion rate of rhodamine**
743 **B**. A) A plot of the surface area of the tubule exposed to the bath versus the net extrusion of
744 rhodamine B for each of the three treatments after 30 minutes of incubation. B) As in 'A' but
745 after 60 minutes. C) As in 'A' but after 90 minutes. Open circles indicate the net extrusion of
746 rhodamine B of individual tubules at a particular time point. Each line with the shaded area
747 around represents the mixed effect model fit with the standard error.

748 **Figure 8. The fluid secretion rate positively influences the net extrusion rate of**
749 **rhodamine B.** A) A plot of the fluid secretion rate versus the net extrusion of rhodamine B for
750 each of the three treatments after 30 minutes of incubation. B) As in 'A' but after 60 minutes.
751 C) As in 'A' but after 90 minutes. Open circles indicate the net extrusion of rhodamine B of
752 individual tubules at a particular time point. Each line with the shaded area around represents
753 the mixed effect model fit with the standard error.

Table 1. Comparison of linear mixed effect models incorporating length, diameter or surface area. Based on the lowest AIC parameter, the surface area was the best explanatory variable for the secretion rate. Only the fixed effects are shown.

model	*df*	*AIC*	*BIC*	*LogLik*	*deviance*
`secretion rate ~ diameter * time + treatment * time`	25	-163.00	-69.75	106.50	-213.00
`secretion rate ~ length * time + treatment * time`	25	-178.10	-84.85	114.05	-228.10
`secretion rate ~ surface * time + treatment * time`	25	**-188.05**	-94.80	119.03	-238.05

Table 2. Outcomes of the linear mixed effect model investigating the effect of surface area, time of incubation, and treatment on the fluid secretion rate of Malpighian tubules. The model applied was (`Secretion rate ~ surface * time + treatment * time + (1| locust) + (1+time|tubule)`).

Predictor (reference)	*ANOVA type II Wald*	*Mean ± SE*	*p*
Intercept (R60, Preincubation, surface = 2 mm^2)		0.55 ± 0.06	**<.001**
Surface	$\chi2$ = 47.44, df=1, **p<.001**	0.27 ± 0.04	**<.001**
Time 30		-0.22 ± 0.04	**<.001**
Time 60	$\chi2$ = 283.94, df=3, **p<.001**	-0.28 ± 0.04	**<.001**
Time 90		-0.29 ± 0.05	**<.001**
Saline x Time 30		-0.09 ± 0.06	.115
Saline x Time 60		-0.17 ± 0.07	**.015**
Saline x Time 90		-0.22 ± 0.08	**.007**
V125 x Time 30		0.04 ± 0.06	.455
V125 x Time 60	$\chi2$ = 23.81, df=9, **p=.005**	-0.02 ± 0.07	.715
V125 x Time 90		-0.05 ± 0.08	.533
V250 x Time 30		-0.17 ± 0.06	**.006**
V250 x Time 60		-0.27 ± 0.07	**<.001**
V250 x Time 90		-0.28 ± 0.08	**.001**

Table 3. Outcomes of the linear mixed effect models for each time interval . The model (`Secretion rate ~ surface + treatment + (1| locust)`) was used to investigate the effect of the tubule surface area (A) and the effect of rhodamine and verapamil (B) on the fluid secretion rate. 'A' shows the estimates of the mean influence of each unit of surface (mm^2) on the fluid secretion rate, whereas 'B' shows the estimates of the mean influence of each treatment on the fluid secretion rate.

		Preincubation		**Time 30**		**Time 60**		**Time 90**	
	Predictor (reference)	*Mean ± SE*	*p*	*Mean ± SE*	*p*	*Mean ± SE*	*p*	*Mean ± SE*	*p*
A	Surface (R60)	0.29 ± 0.05	**<.001**	0.20 ± 0.03	**<.001**	0.15 ± 0.02	**<.001**	0.16 ± 0.04	**<.001**
	Surface (Saline)	0.29 ± 0.05	**<.001**	0.20 ± 0.03	**<.001**	0.15 ± 0.02	**<.001**	0.17 ± 0.04	**<.001**
	Surface (V125)	0.29 ± 0.05	**<.001**	0.20 ± 0.03	**<.001**	0.15 ± 0.02	**<.001**	0.15 ± 0.05	**.002**
	Surface (V250)	0.29 ± 0.05	**<.001**	0.20 ± 0.03	**<.001**	0.15 ± 0.02	**<.001**	0.02 ± 0.04	.512
B	Intercept (R60, surface=2)	0.55 ± 0.09		0.33 ± 0.06		0.27 ± 0.04		0.25 ± 0.04	
	Saline (R60)	0.24 ± 0.13	.070	0.14 ± 0.10	.136	0.07 ± 0.06	.242	0.02 ± 0.06	.751
	V125 (R60)	-0.02 ± 0.13	.908	0.03 ± 0.10	.756	-0.04 ± 0.06	.557	-0.07 ± 0.06	.280
	V250 (R60)	0.20 ± 0.13	.133	-0.02 ± 0.10	.800	-0.12 ± 0.06	.052	-0.10 ± 0.06	.101

Table 4. The outcomes of linear mixed effect model used to investigate the effect of incubation time and treatment on the rhodamine concentration of the droplets secreted. The model applied was (`Rhodamine concentration ~ secretion rate * time + treatment * time + (1| locust) + (1+time|tubule)`).

Predictor (reference)	*ANOVA type II Wald*	*Mean ± SE*	*p*
Intercept (R60, SR=0.3, time 30)		59.58 ± 6.66	**<0.001**
Time 60	$\chi2$ = 259.29, df=2, **p<.001**	154.87 ± 10.81	**<0.001**
Time 90		296.43 ± 18.57	**<0.001**
V125 x time 30	$\chi2$ = 85.32, df=4, **p<.001**	-115.11 ± 16.41	**<0.001**
V125 x time 60		-226.53 ± 28.08	**<0.001**
V250 x time 30		-103.03 ± 16.69	**<0.001**
V250 x time 60		-215.12 ± 28.66	**<0.001**

Table 5. Outcomes of the linear mixed effect models for each time interval upon the concentration of rhodamine within the secreted droplets. The model (`Rhodamine concentration ~ secretion rate + treatment + (1| locust)`) was used to investigate the effect of rhodamine and verapamil in the treatment bath upon the concentration of rhodamine in the droplets secreted after each interval of time.

	Time 30		**Time 60**		**Time 90**	
Predictor (reference)	*Mean ± SE*	*p*	*Mean ± SE*	*p*	*Mean ± SE*	*p*
Intercept (R60)	59.4 ± 4.9		215.7 ± 13.5		359.2 ± 21.7	
V125 (R60)	-48.9 ± 7.6	**<.001**	-163.7 ± 20.5	**<.001**	-273.0 ± 32.7	**<.001**
V250 (R60)	-48.2 ± 7.5	**<.001**	-151.9 ± 21.2	**<.001**	-256.6 ± 33.7	**<.001**
V250 (V125)	0.7 ± 8.0	.931	11.8 ± 22.6	.605	16.4 ± 35.4	.644

Table 6. Outcomes of a linear mixed effect model to investigate the effect of incubation time and treatment on the quantity of rhodamine extruded in the droplets secreted. The model applied was (`Net extrusion of rhodamine ~ surface * time * treatment + (1| locust) + (1+time|tubule)`).

Predictors	*ANOVA type II Wald*	*Mean ± SE*	*p*
Intercept (R60, surface=2, time 30)		18.75 ± 2.3	**<0.001**
time 60	$\chi2$ = 153.17, df=2, **p<.001**	36.11 ± 2.87	**<0.001**
time 90		61.67 ± 4.8	**<0.001**
Surface x V125 x time 60	$\chi2$ = 11.36, df=4, **p=.023**	-15.98 ± 7.11	**0.025**
Surface x V250 x time 60		-16.11 ± 6.76	**0.017**
Surface x V125 x time 90		-29.75 ± 11.89	**0.012**
Surface x V250 x time 90		-34.14 ± 11.28	**0.002**

Table 7. Outcomes of a linear mixed effects model investigating the effect of treatment and tubule surface area on the quantity of rhodamine extruded in the droplets secreted at each time interval. The model applied was (`Net extrusion of rhodamine ~ surface * treatment + (1| locust)`). (A) Shows the effect of rhodamine and verapamil on the quantity of rhodamine extruded in the droplets secreted. (B) As in 'A' but showing the effect of the tubule surface area.

		Time 30		**Time 60**		**Time 90**	
	Predictor (reference)	*Mean ± SE*	*p*	*Mean ± SE*	*p*	*Mean ± SE*	*p*
A	Intercept (R60, surface=2)	18.8 ± 2.6		54.7 ± 7.3		80.3 ± 9.3	
	V125 (R60)	-15.8 ± 4.0	**<.001**	-42.4 ± 11.3	**<.001**	-61.4 ± 14.5	**<.001**
	V250 (R60)	-17.2 ± 4.0	**<.001**	-43.4 ± 11.3	**<.001**	-59.1 ± 14.4	**<.001**
	V250 (V125)	-1.4 ± 4.2	.736	-1.1 ± 12.3	.931	2.3 ± 15.6	.884
B	Surface (R60)	2.11 ± 1.77	.231	33.05 ± 7.25	**<.001**	51.37 ± 8.61	**<.001**
	Surface (V125)	2.11 ± 1.77	.231	6.79 ± 9.10	.456	11.45 ± 10.80	.289
	Surface (V250)	2.11 ± 1.77	.231	5.20 ± 6.98	.457	3.91 ± 8.12	.630

Table 8. Outcomes of the linear mixed effects model for each time interval to investigate the effect of the secretion rate on the quantity of rhodamine extruded in the droplets secreted. The model applied was (`Net extrusion of rhodamine ~ secretion rate * treatment + (1| locust)`). The means estimate the influence of each nL/min of secretion rate on the quantity of rhodamine extruded.

	Time 30		**Time 60**		**Time 90**	
Predictor (reference)	*Mean ± SE*	*p*	*Mean ± SE*	*p*	*Mean ± SE*	*p*
Secretion rate (R60)	62.07 ± 6.12	**<.001**	235.76 ± 13.73	**<.001**	272.40 ± 19.35	**<.001**
Secretion rate (V125)	7.47 ± 6.27	.234	51.72 ± 16.71	**.002**	82.93 ± 34.60	**.017**
Secretion rate (V250)	-1.16 ± 4.56	.800	58.81 ± 16.00	**<.001**	125.53 ± 33.72	**<.001**

Table 9. Summary of the mean values of secretion rate, rhodamine concentration and net extrusion of rhodamine for each treatment at each time point.

	Treatment	**Preincubation**	**Time 30**	**Time 60**	**Time 90**	**SR difference % between preincubation and Time 90**
		Mean ± SE	*Mean ± SE*	*Mean ± SE*	*Mean ± SE*	
Fluid secretion rate (nL/min)	R60	0.55 ± 0.09	0.33 ± 0.06	0.27 ± 0.04	0.25 ± 0.04	-55%
	Saline	0.78 ± 0.10	0.47 ± 0.07	0.34 ± 0.05	0.27 ± 0.05	-65%
	V125	0.53 ± 0.10	0.36 ± 0.07	0.23 ± 0.05	0.19 ± 0.05	-64%
	V250	0.75 ± 0.10	0.30 ± 0.07	0.14 ± 0.05	0.15 ± 0.05	-80%
Rho concentration (μM)	R60		59.4 ± 4.9	215.7 ± 13.5	359.2 ± 21.7	
	V125		10.5 ± 5.8	52.0 ± 15.6	86.1 ± 25.6	
	V250		11.19 ± 5.7	63.8 ± 17.0	102.6 ± 27.7	
Net extrusion of Rho (fmol/min)	R60		18.8 ± 2.6	54.7 ± 7.3	80.3 ± 9.3	
	V125		3.0 ± 3.0	12.4 ± 8.7	18.9 ± 11.1	
	V250		1.6 ± 3.0	11.3 ± 8.7	21.2 ± 11.0	
	Net P-glycoprotein contribution		**17.2 (91%)**	**43.4 (79%)**	**59.1 (74%)**	**Total: 119.7 (78%)**

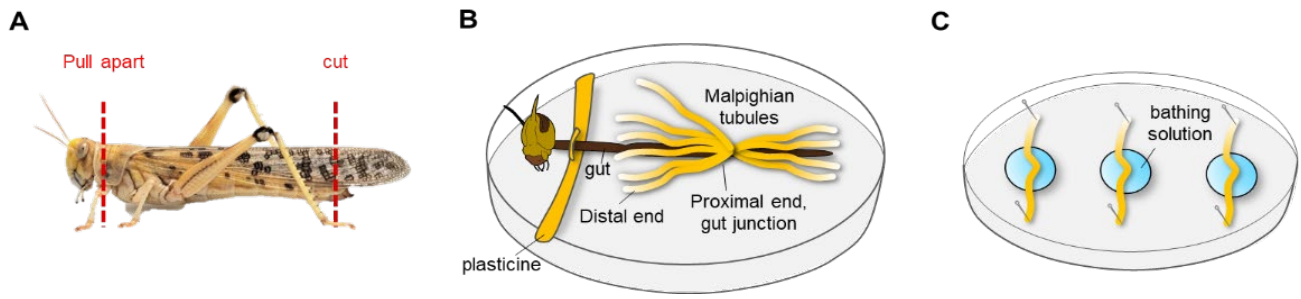

Figure 1. The extraction and preparation of Malpighian tubules for *ex vivo* experimentation from the desert locust, *Schistocerca gregaria*. A) Cutting the anterior tip of the abdomen permits removal of the head and the fully intact gut. B) The gut is submerged in saline and the Malpighian tubules are exposed. The head is separated from the saline bath by a barrier of modelling clay. C) Three tubules are removed from each locust and fixed on a Sylgard® surface traversing a small drop of bathing solution, and covered with paraffin oil.

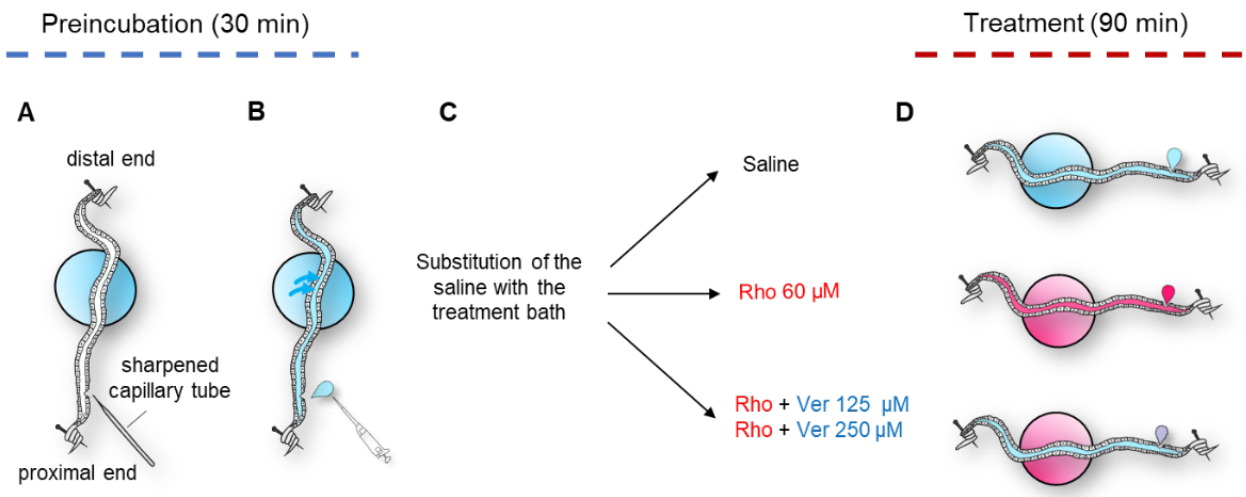

Figure 2. The experimental scheme for assaying the presence of P-glycoproteins within the Malpighian tubules of the desert locust. A) Individual tubules are severed from the gut and the proximal and distal ends of the tubule are wound around Minuten pins to fix them. Once the saline bath and paraffin oil have been applied, the proximal end of the tubule is punctured with a sharpened capillary tube. B) After 30 minutes of preincubation in saline bath the droplet was removed. C) The saline bath was replaced by a bath containing one of the treatments. D) Every 30 minutes the secreted droplet was removed, placed on the Petri dish and photographed.

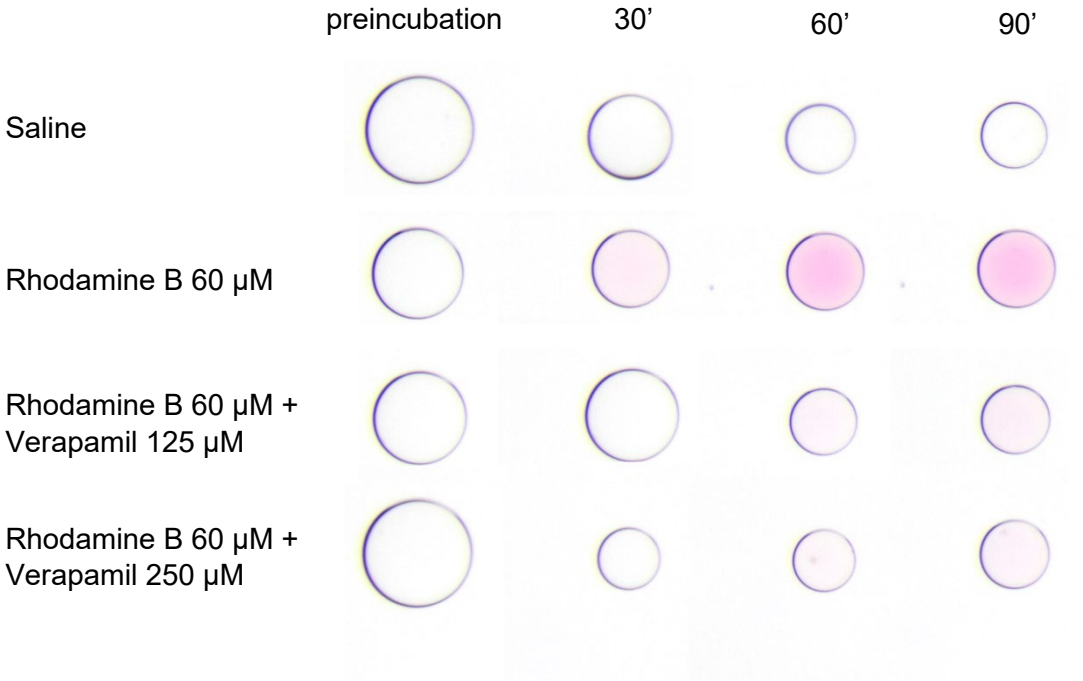

Figure 3. Examples of the droplets secreted by the Malpighian tubules of desert locusts during preincubation in saline and at every 30 minutes in each of the different treatments. The size of each droplet depends upon the fluid secretion rate whilst the colour is determined by the net extrusion rate.

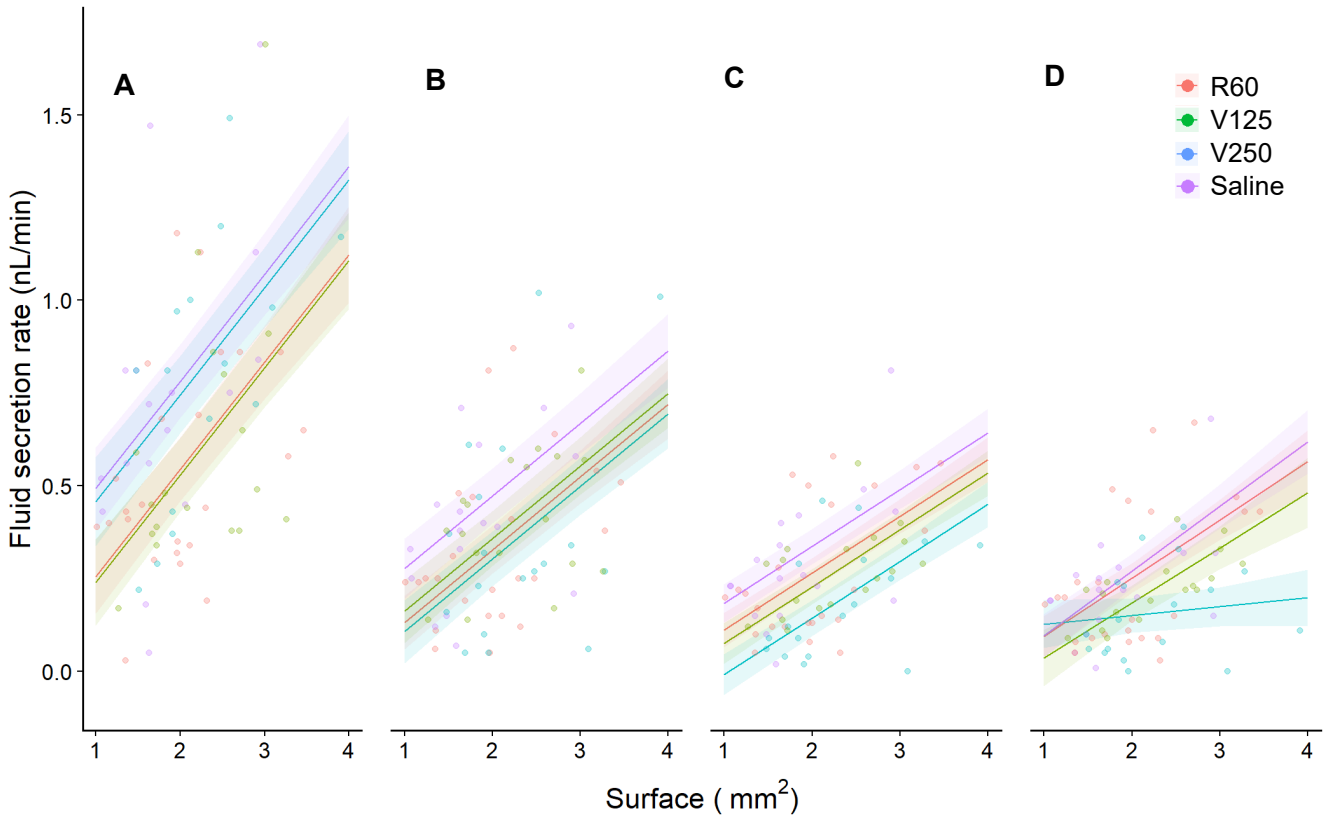

Figure 4. Tubule surface area positively influences the fluid secretion rate. A) A plot of the surface area of the tubule exposed to the bath versus the fluid secretion rate for each of the four treatments during preincubation. B) As in 'A' but 30 minutes after the saline bath was replaced by one of the four treatment baths. C) As in 'B' but after 60 minutes. D) As in 'B' but after 90 minutes. Open circles indicate the fluid secretion rates of individual tubules at a particular time point. Each line with the shaded area around represents the mixed effect model fit with the standard error.

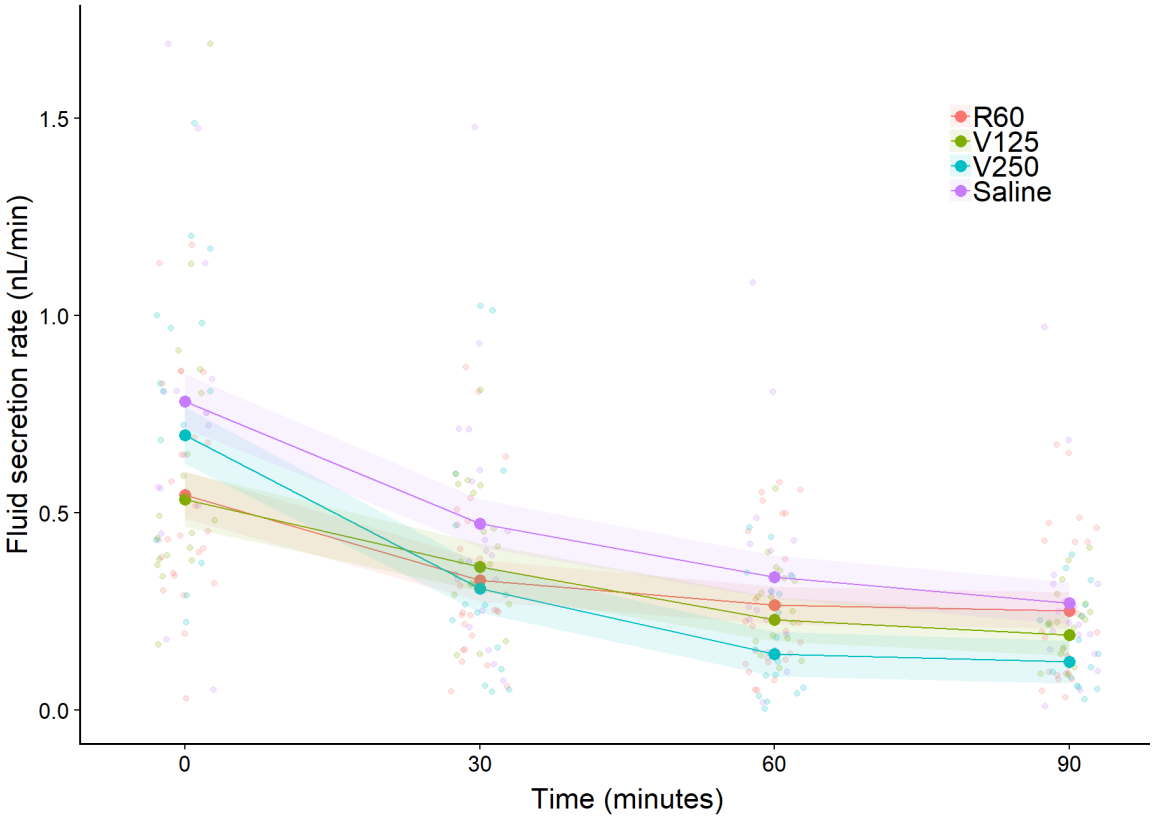

Figure 5. The mean fluid secretion rate of Malpighian decreased with time in all the treatments. A plot of the time from the replacement of the preincubation saline bath with one of the four treatments. Open circles indicate the fluid secretion rates of individual tubules at a particular time point. Each line with the shaded area around represents the mixed effect model fit with the standard error.

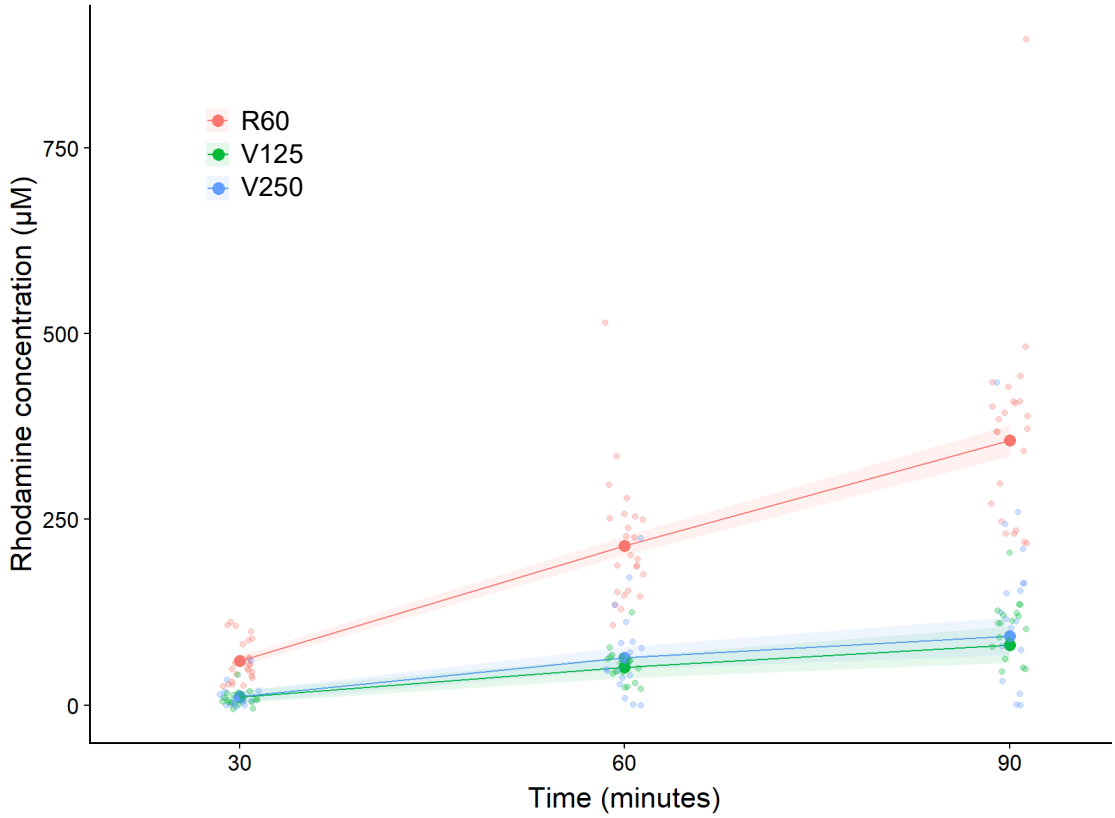

Figure 6. The mean rhodamine B concentration of the droplets secreted by the Malpighian tubules increased over time in all the treatments. The addition of verapamil (125 or 250 µM) reduced the rhodamine concentration of the droplets secreted compared with the control treatment 60 µM rhodamine. Open circles indicate the rhodamine concentration of the droplets secreted by individual tubules at a particular time point. Each line with shaded region represents the mixed effect model fit with the standard error.

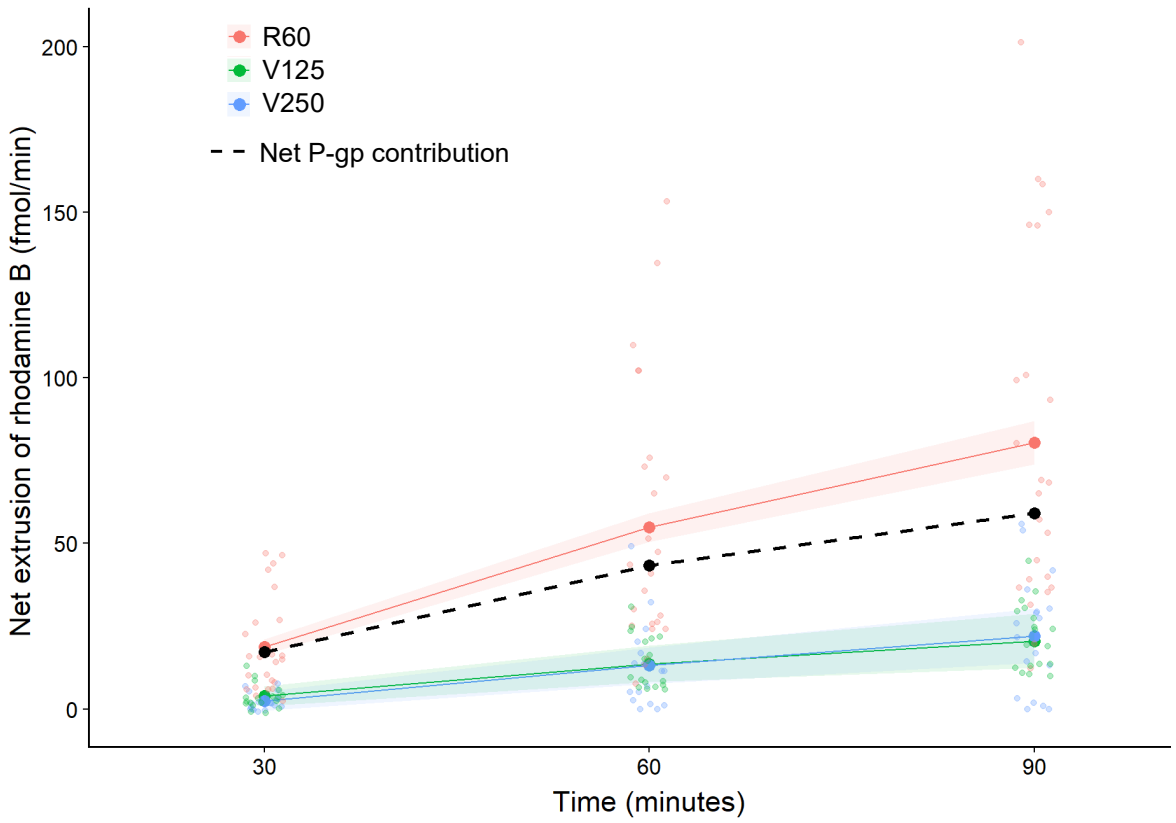

Figure 7. The mean net extrusion of rhodamine B increased over time in all the treatments. The addition of verapamil (125 μM or 250 μM) reduced the net extrusion of rhodamine B compared with the control treatment 60 μM Rhodamine. Open circles indicate the net extrusion of rhodamine B by individual tubules at a particular time point. Each line with shaded region represents the mixed effect model fit with the standard error. The dashed line represents the net contribution of the P-glycoproteins obtained by subtracting the net extrusion of rhodamine in the V250 treatment from the R60.

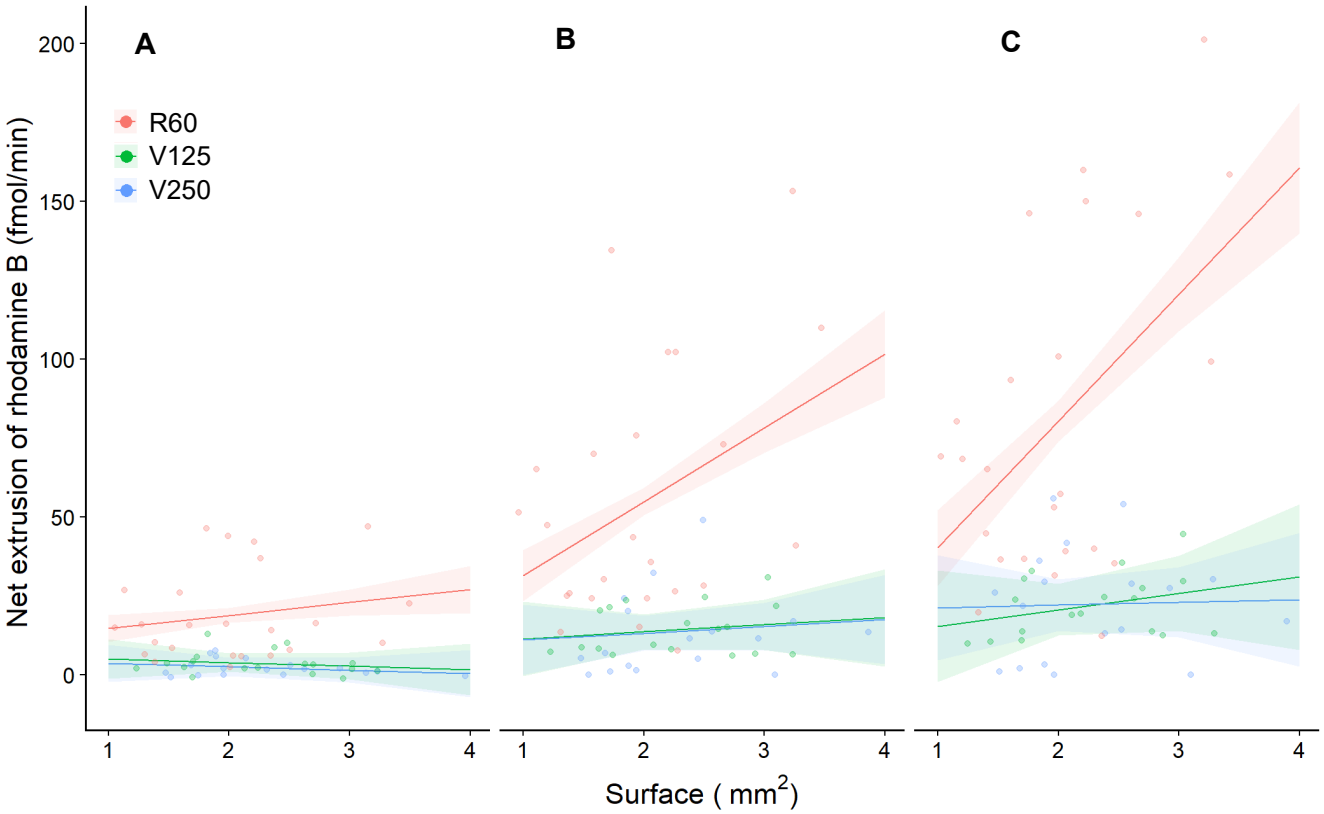

Figure 8. Tubule surface area positively influences the net extrusion of rhodamine B. A) A plot of the surface area of the tubule exposed to the bath versus the net extrusion of rhodamine B for each of the three treatments after 30 minutes of incubation. B) As in 'A' but after 60 minutes. C) As in 'A' but after 90 minutes. Open circles indicate the net extrusion of rhodamine B of individual tubules at a particular time point. Each line with the shaded area around represents the mixed effect model fit with the standard error.

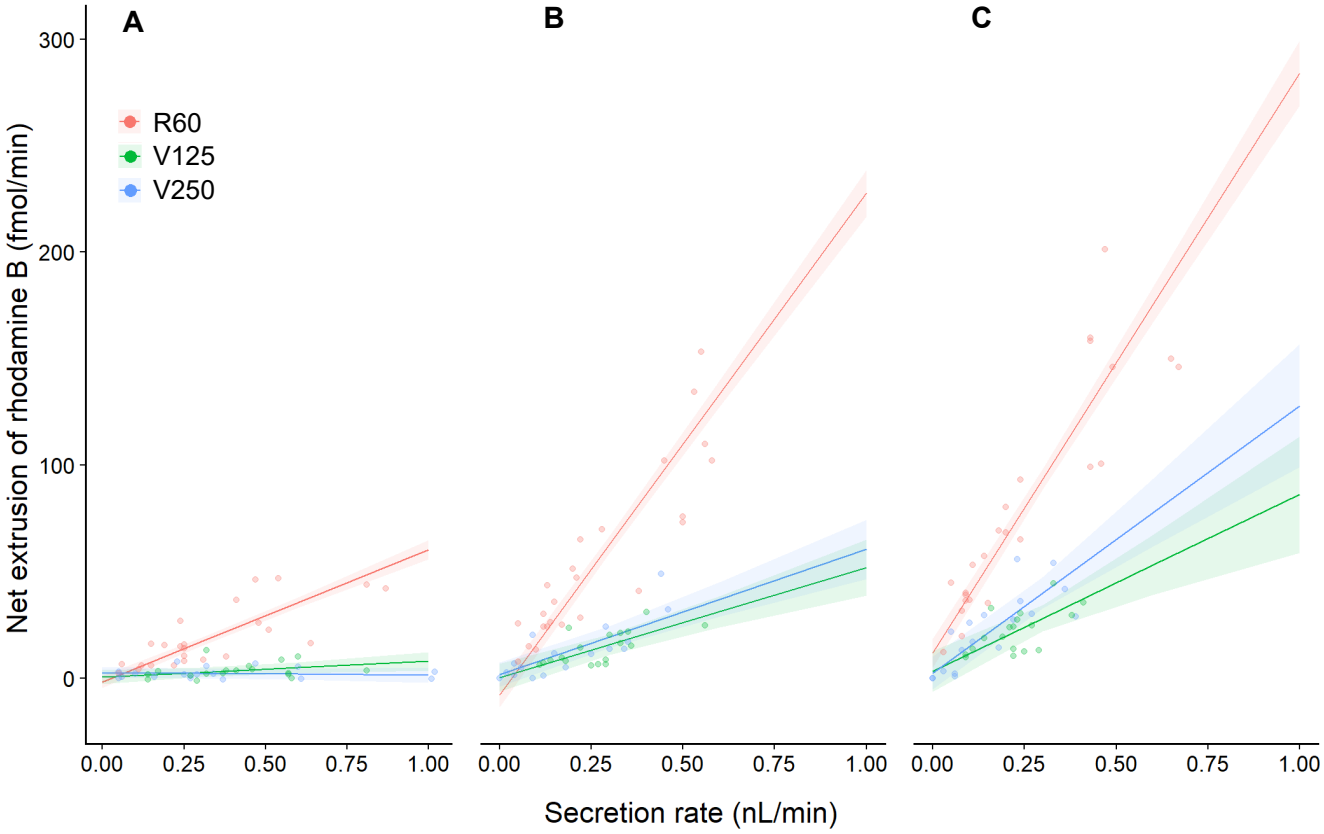

Figure 9. The fluid secretion rate positively influences the net extrusion of rhodamine B. A) A plot of the fluid secretion rate versus the net extrusion of rhodamine B for each of the three treatments after 30 minutes of incubation. B) As in 'A' but after 60 minutes. C) As in 'A' but after 90 minutes. Open circles indicate the net extrusion of rhodamine B of individual tubules at a particular time point. Each line with the shaded area around represents the mixed effect model fit with the standard error.